Clim Dyn
DOI 10.1007/s00382-011-1035-z

AMOC variations in 1979–2008 simulated by NCEP operational ocean data assimilation system

Boyin Huang · Yan Xue · Arun Kumar · David W. Behringer

Received: 29 July 2010 / Accepted: 13 February 2011

Abstract Variations in the Atlantic meridional overturning circulation (AMOC) between 1979 and 2008 are documented using the operational ocean analysis, the Global Ocean Data Assimilation System (GODAS), at the National Centers for Climate Prediction (NCEP). The maximum AMOC at 40°N is about 16 Sv in average with peak-to-peak variability of 3–4 Sv. The AMOC variations are dominated by an upward trend from 1980 to 1995, and a downward trend from 1995 to 2008. The maximum AMOC at 26.5°N is slightly weaker than hydrographic estimates and observations from mooring array. The dominant variability of the AMOC in 20°–65°N (the first EOF, 51% variance) is highly correlated with that in the subsurface temperature (the first EOF, 33% variance), and therefore, with density (the first EOF, 25% variance) in the North Atlantic, and is consistent with the observational estimates based on the World Ocean Database 2005. The dominant variabilities of AMOC and subsurface temperature are also analyzed in the context of possible links with the net surface heat flux, deep convection, western boundary current, and subpolar gyre. Variation in the net surface heat flux is further linked to the North Atlantic Oscillation (NAO) index which is found to lead AMOC variations by about 5 years. Our results indicate that AMOC variations can be documented based on an ocean analysis system such as GODAS.

Keywords Atlantic meridional overturning circulation · AMOC · Global ocean data assimilation system · GODAS · North Atlantic oscillation · NAO · National centers for environmental prediction · NCEP

1 Introduction

The Atlantic Meridional Overturning Circulation (AMOC) is composed of a net northward flow of warm water in the upper approximately 1 km of the ocean and a net southward flow of cold water in the deeper ocean. The AMOC carries up to 25% of the northward global atmosphere–ocean heat transport in the northern hemisphere (Wunsch 2005). Monitoring and understanding the AMOC variations are of importance under several contexts. For example, under the purview of the Intergovernmental Panel on Climate Change (IPCC) 5th assessment efforts, plans are underway for initializing climate models to improve their decadal predictions of climate variability (Meehl et al. 2009) with the underlying assumption that the skills for climate prediction can be enhanced by a suitable initialization in the ocean and atmosphere (Smith et al. 2007; Keenlyside et al. 2008; Pohlmann et al. 2009). Understanding AMOC variation is also of importance for quantifying and assessing the potential for abrupt climate change that may result from the warming and freshening related to the sea-ice melting in the North Atlantic (Kuhlbrodt et al. 2007; and references therein). Finally, manifestation of AMOC variability in sea surface temperatures (SSTs; Knight et al. 2005), although not well agreed upon, could also have impacts on the global terrestrial climate (Held et al. 2005).

B. Huang · Y. Xue · A. Kumar
Climate Prediction Center, NOAA,
Camp Springs, MD, USA

D. W. Behringer
Environmental Modeling Center,
NOAA, Camp Springs, MD, USA

B. Huang (✉)
National Climate Data Center, Asheville,
NC 28801, USA
e-mail: boyin.huang@noaa.gov

Published online: 01 March 2011

AMOC variations have been estimated based on sparse in situ observations. Bryden et al. (2005) estimated the AMOC intensity at 25°N from five hydrographic sections between 1957 and 2004, and found a slowing AMOC of 6 Sv during the period. However, such low-frequency variability in the AMOC is likely aliased by intra-annual variability (Kanzow et al. 2010). The problem is being addressed by the continuous monitoring of the AMOC at 26.5°N that began in April 2004 with the installation of a trans-Atlantic mooring array. Using the data from the mooring array between April 2004 and March 2005, Cunningham et al. (2007) demonstrated a large seasonal variability of the AMOC with a standard deviation of 5.6 Sv upon a mean of 18.7 Sv.

AMOC variations can also be reconstructed using ocean data assimilation systems. The ocean synthesis from the "Estimating the Circulation and Climate of the Ocean (ECCO)" project suggests that the AMOC slowed down from 1993 to 2004, at the rate of 0.19 Sv per year (Wunsch and Heimbach 2006). The reconstruction of the AMOC for the period 1959–2006 from the European Centre for Medium-Ranged Weather Forecast (ECMWF) operational analysis (Balmaseda et al. 2007) agrees well with previous observed estimations and suggests a downward trend from 1995 to 2006. The ocean synthesis from German contribution to the Estimating the Circulation and Climate of the Ocean Project (GECCO) suggests a steady increase of the AMOC, by approximately 4 Sv, from the 1960s to the mid-1990s, followed by a short period of decline (Köhl and Stammer 2007). Häkkinen and Rhines (2004) attributed this reduction of the AMOC after 1995 to the weakening of the subpolar gyre, characterized by a decrease in sea surface height observed from satellite altimetry. Böning et al. (2006) further suggested that the changes in the subpolar gyre are highly correlated with the deep western boundary current off Labrador, which is then connected to the variations of the AMOC in the subtropical North Atlantic. The analysis also indicated that the decadal variability of the subpolar gyre and AMOC near 48°N is largely driven by changes in both heat flux and wind stress associated with the North Atlantic Oscillation (NAO) (Böning et al. 2006; Eden and Willebrand 2001).

Despite some agreements found among the AMOC estimations in the ocean synthesis products discussed above, it is hard to quantify uncertainties in the AMOC estimates due to the sparse observed data. To address this issue a continuous monitoring of the AMOC variations using different ocean synthesis products may be a feasible alternative, although an assessment of AMOC variability in the ocean analysis systems is first required to build confidence in such products. In the present analysis the AMOC variability is documented based on the Global Ocean Data Assimilation System (GODAS) operational at the National Centers for Environmental Prediction (NCEP; Behringer and Xue 2004).

We will first briefly describe the GODAS and the analysis procedure in Sect. 2, followed by description of the AMOC variability of the GODAS and comparison with observations in Sect. 3. We will discuss how the AMOC variations in the GODAS are associated with variations in temperature and salinity, as well as the density (Sect. 4). Variations of the AMOC are further associated with changes in buoyancy fluxes, deep convection, western boundary currents, and subpolar gyre in Sect. 5. Section 6 is the summary and discussions.

2 GODAS outputs and analysis procedures

The ocean model in GODAS is based on the Geophysical Fluid Dynamics Laboratory (GFDL) Modular Ocean Model (MOM) version 3 in a quasi-global (75°S–65°N) configuration (no sea-ice variability is included). The zonal resolution is 1°. The meridional resolution is 1/3° between 10°S and 10°N, gradually increasing through the tropics to 1° poleward of 30°S and 30°N. There are 40 layers in the vertical with 27 layers in the upper 400 m of the ocean, and the maximum depth is approximately 4.5 km. The vertical resolution is 10 m from the surface to 240 m depth, gradually increasing to about 511 m in the bottom layer. The GODAS is forced with the NCEP/Department of Energy (DOE) atmospheric reanalysis fluxes (Reanalysis 2 hereafter, Kanamitsu et al. 2002). GODAS uses the 3-dimensional variational (3D-VAR) (Behringer et al. 1998; Behringer 2007) scheme to assimilate temperature profiles from expendable bathythermographs (XBTs), Tropical Atmosphere Ocean (TAO) and Triangle Trans Ocean Buoy Network (TRITON), Pilot Research Moored Array (PIRATA), and Argo profiling floats. Only the temperature data in the top 750 m are assimilated into the GODAS. Due to the lack of direct salinity observations, synthetic salinity profiles constructed from temperature and a local T-S climatological relationship are also assimilated. More detailed descriptions of the data assimilation procedure can be found in Behringer and Xue (2004) and Huang et al. (2008). Since GODAS is an operational system, it is potentially useful in monitoring and assessing the AMOC variations in real time.

To assess the impacts of observed salinity on the AMOC simulation, we also analyze an additional simulation (referred to as GODAS_SAL) that assimilates observed salinity in addition to observed temperature during the Argo period from 2001 to 2006. The model-simulated AMOC variability, where feasible, are compared with available observational estimate.

An empirical orthogonal function (EOF) analysis is used to assess the dominant variability in temperature and

density in the GODAS. To concentrate on the *variability* alone, the linear trend in temperature and density is first removed at each grid point before the EOF analysis. Temperature and density are zonally averaged in the Atlantic basin, and are regrided to a uniform 1° in latitude and 20 m in depth. The EOF analysis is based on the annually averaged anomalies between 20° and 65°N from the surface to 700 m in depth for 1979–2008. The dominant EOFs and principal component (PCs) of the GODAS are compared with those of the World Ocean Database 2005 (WOD05; Boyer et al. 2006). In the WOD05, temperature is annually averaged in 1979–2008 and salinity is filtered with a 5-year running mean in 1979–2004.

Similarly, the EOFs of the AMOC are derived with the annually averaged anomalies between 20° and 65°N from the surface to 4,000 m in depth. The dominant variability of the AMOC, the first PC (PC1), is analyzed and compared with the PC1s of temperature and density anomalies. As the anomalous meridional density gradient between the subpolar (50°–65°N) and subtropical (30°–45°N) Atlantic is found to be closely related to the PC1 of the AMOC, we also analyze the relative contributions of temperature and salinity to the variation of density gradient.

To understand the forcing mechanisms for the AMOC variability, we calculate the EOFs of annual anomalies of the net surface heat flux, freshwater flux, and Ekman pumping. We further relate their dominant variability (PC1) with the wintertime (January-March) North Atlantic Oscillation index (NAO) downloaded from http://www.cpc.ncep.noaa.gov/products/precip/CWlink/pna/nao.shtml. The buoyancy forcings from surface heat flux and freshwater flux are also discussed. To further validate the AMOC variability in the GODAS, we analyze how well the GODAS simulates the variability in deep convection, subpolar gyre transport and western boundary currents and their lead/lag correlations with the AMOC.

3 The AMOC variability in the GODAS

The mean strength of the AMOC in the GODAS, calculated between 1979 and 2008, is approximately 16 Sv near 35°N and at 1,000 m depth (Fig. 1a). Spatially coherent variation of the AMOC is quantified based on the EOF analysis between 20° and 65°N from the surface to 4,000 m. The first EOF (EOF1; Fig. 1b) explains 51% of total variance. The largest amplitude for the EOF1 (4 Sv) is located near 44°N and 1,500 m, deeper and to the north of maximum AMOC shown in Fig. 1a. The corresponding PC1 time-series shows a strengthening in the AMOC from 1982 to 1993 and a weakening from 1995 to 2008 (Fig. 1c). This is in phase with the fluctuations of the AMOC at 44°N where maximum for the EOF1 is located.

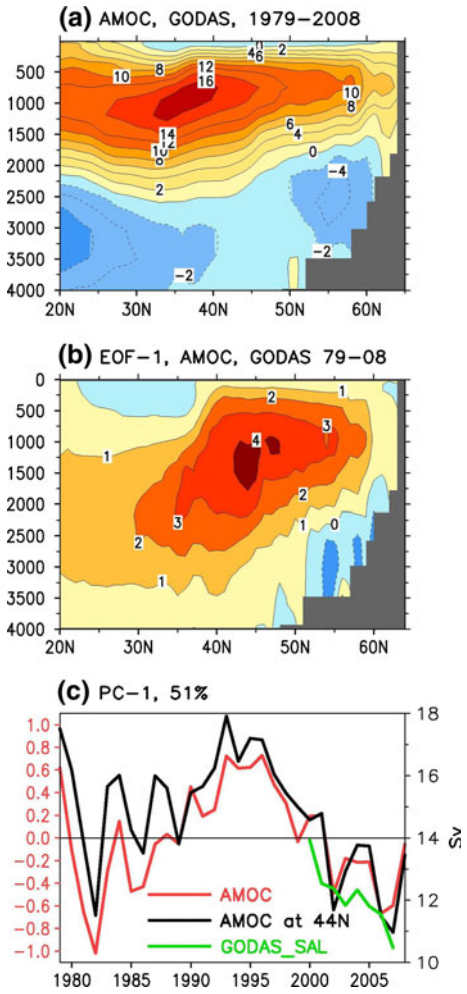

Fig. 1 AMOC in GODAS. **a** Mean (1979–2008). **b** EOF1. The first EOF represents 51% total variance. **c** Normalized PC1, along with the maximum AMOC at 44°N (*right axis*). Contour intervals are 2 Sv in (**a**) and 1 Sv in (**b**). GODAS_SAL in (**c**) results from projecting AMOC in GODAS_SAL onto the EOF1 of AMOC in GODAS

The magnitude and temporal variation of AMOC in the GODAS is largely consistent with results from other model simulations (Balmaseda et al. 2007; Frankignoul et al. 2009). The sharp decline of the AMOC from 1979 to 1982 might be unrealistic and is likely related to a model spin up issues.

Figure 2a shows the annually averaged maximum AMOC at 26.5°N from the GODAS, GODAS_SAL, and observations. The AMOC in the standard GODAS has a downward trend from 1979 to 1986, and an upward trend from 1986 to 2004 overlain with significant interannual variability (Fig. 2a). This is different from a downward trend in Balmaseda et al. (2007).

For observational counterpart, four hydrographic data based estimates at 25°N (Bryden et al. 2005) show a weak upward trend from 1981 to 1993, and a strong downward trend from 1993 to 2004. Kanzow et al. (2010) pointed out

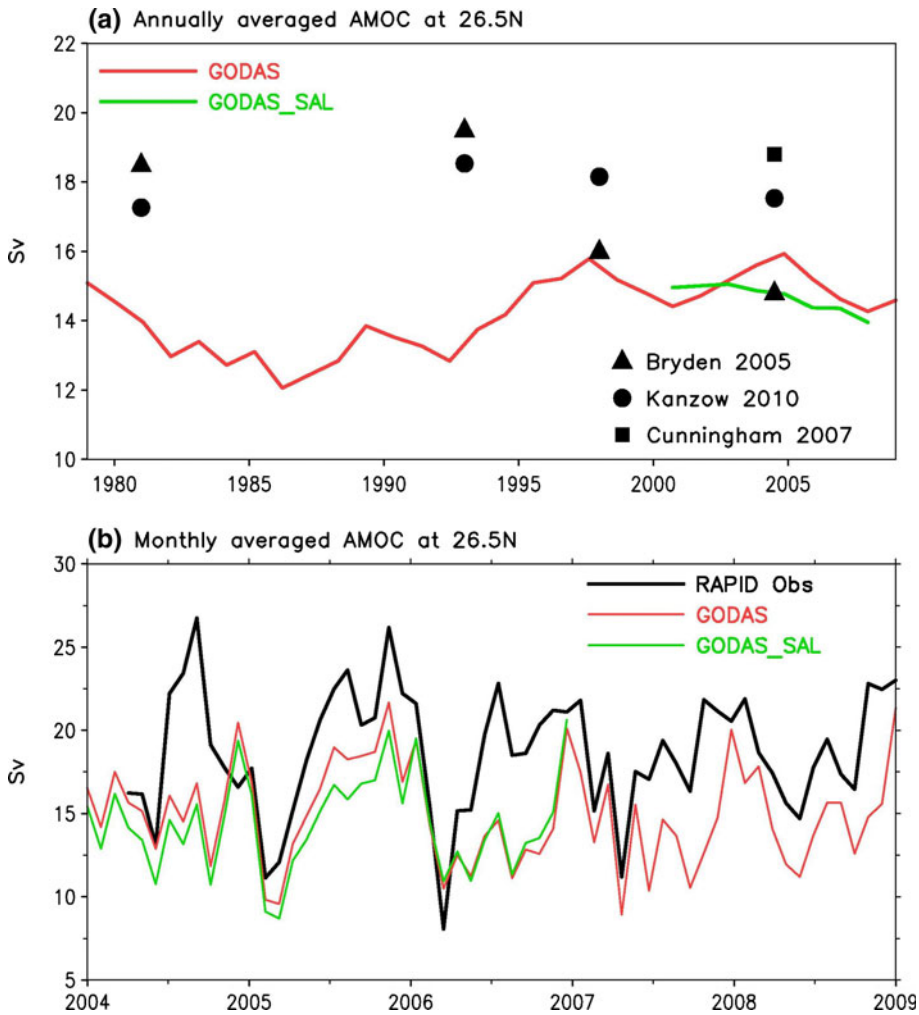

Fig. 2 **a** Annually averaged maximum AMOC (unit: Sv) at 26.5°N in GODAS, and GODAS_SAL, along with observed AMOC anomalies by Bryden et al. (2005, *filled triangle*) and Kanzow et al. (2010, *filled circle*) at 25°N and by Cunningham et al. (2007, *filled square*) at 26.5°N. A 3-year running mean is applied. **b** Monthly AMOC at 26.5°N from RAPID observations, GODAS and GODAS_SAL. The correlation coefficients are 0.67 (0.64), respectively, between RAPID and GODAS (GODAS_SAL). The Standard deviation (STD) is 1.4 for GODAS in (**a**); and 3.7, 3.0, and 2.8 Sv, respectively in RAPID, GODAS, and GODAS_SAL in (**b**)

that estimates based on episodic observations can be contaminated by aliasing due to the seasonal cycle. After removing the aliasing due to the seasonal cycle from the estimates of Bryden et al. (2005), the weak upward trend from 1981 to 1993 remains unchanged, but the downward trend from 1993 to 2004 is significantly reduced (Kanzow et al. 2010). The seasonal correction by Kanzow et al. (2010) is 2–4 Sv. In comparison to these observations, the AMOC strength in the GODAS appears too weak, particularly before 1997. Further, the downward trend from 1997 to 2008 in GODAS is not as evident as in the observed estimates (Kanzow et al. 2010). The downward trend from 1979 to 1986 in the GODAS cannot directly be validated by the observed estimates due to their sparse temporal resolution.

On intra-annual timescale, the variations of the AMOC in the GODAS at 26.5°N are largely in agreement with observations. Figure 2b shows the monthly averaged maximum AMOC at 26.5°N from Rapid Climate Change (RAPID; http://www.bodc.ac.uk/rapidmoc) mooring array (Kanzow et al. 2010) and GODAS between 2004 and 2008. It is clear that the observed variations of AMOC at 26.5°N are well captured in the GODAS with a correlation coefficient of 0.67. However, its magnitude and variability are somewhat underestimated. Between 2004 and 2008, mean and standard deviation, respectively, are 18.7 and 3.7 Sv in RAPID, and 14.9 and 3.0 Sv in GODAS. In addition, RAPID observations (Fig. 2b) indicate that the standard deviation of AMOC at 26°N between 2004 and 2008 (3.7 Sv) is weaker than that in the early period between 2003 and 2004 (5.6 Sv; Cunningham et al. 2007). The larger standard deviation in Cunningham et al. (2007) may partly be attributed to the use of daily averaged data.

4 The roles of temperature and salinity change in the AMOC variability

EOFs and PCs of annually anomalous temperature and density between 20° and 65°N from the surface to 700 m are analyzed separately to understand the roles of temperature and density in the AMOC variations. The first EOF

and PC (Fig. 3a, c) show that, superimposed on major interannual fluctuations, zonally averaged temperature exhibited an anomalous cooling north of 45°N and an anomalous warming between 25° and 45°N from 1979 to 1994, and an opposite tendency from 1994 to 2008. This temperature variability represents 33% of total variance, and is a dominant contribution to the density variability (Fig. 3b, d). The EOF1 of density represents 25% of total variance.

It is clear that the variations of temperature (Fig. 3c) and density (Fig. 3d) are in phase with the AMOC PC1 (Fig. 1c) on low-frequency time scales. Their respective correlation with the AMOC PC1 is 0.60 and 0.65. These results indicate that the variation of the AMOC PC1 is associated with changes in density (Grist et al. 2009; Josey et al. 2009). Density increased north of 45°N and decreased south of 45°N from 1979 to 1995, and had opposite changes from 1995 to 2008. Therefore, the meridional gradient of density between subpolar (50°–65°N) and subtropical (30°–45°N) Atlantic strengthened from 1979 to 1995 and weakened from 1995 to 2008 (Fig. 4). The strengthening (weakening) of meridional gradient of density is compatible with the corresponding strengthening (weakening) of the AMOC from 1980 to 1995 (from 1995 to 2008), and is consistent with studies of Vellinga (1996) and Wang et al. (2009). The density structure (Fig. 3b) favors a stronger change in AMOC near 45°N. This may explain why AMOC PC1 is well correlated with maximum AMOC at 45°C, but less correlated at 26°N. Therefore, we refer AMOC as the AMOC PC1 or maximum AMOC at 45°N in our following discussions.

Variations of temperature and density in the GODAS are concordant with observed analyses of WOD05. Figure 5a, c show the first EOF and PC of annually anomalous temperature in the WOD05, which are very similar to those simulated in the GODAS (Fig. 3a, c) with correlation coefficients of 0.81 and 0.80 in EOF1 and PC1, respectively. However, the interannual variability of temperature is slightly overestimated in the GODAS than in the WOD05, e.g. during 1986–1991. The EOF loading of temperature is vertically more homogeneous in the GODAS than in the WOD05.

For density, the EOF1 and PC1 of the GODAS (WOD05) are derived with annual (5-year running mean) anomalies of temperature and salinity. The maximum EOF1 loadings in the GODAS are located near the surface at 50° and 35°N (Fig. 3b), while they are located near the surface at 55°N and near 600 m at 37°N (Fig. 5b) in the WOD05. The density variation leads the AMOC by approximately 1–2 year in the WOD05 (Fig. 5d) while it is in phase in the GODAS (Fig. 3d). The first EOF and PC of density in the WOD05 are correlated with those in the GODAS; and respective correlation coefficients are 0.68 and 0.58. The variances explained by the first EOFs of temperature and density are higher in the WOD05 (43 and 39%, respectively) than in the GODAS (33, and 25%, respectively).

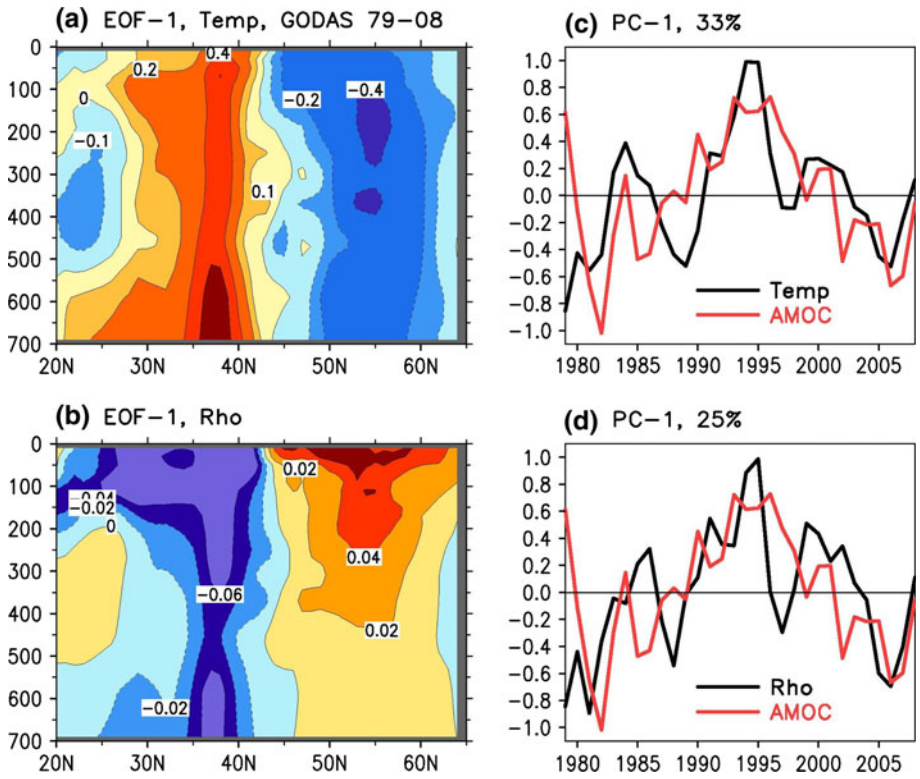

Fig. 3 First EOF of de-trended, basin-averaged, and annually anomalous (**a**) temperature and (**b**) density in the Atlantic in GODAS. Normalized first PC of (**c**) temperature and (**d**) density in the Atlantic, along with normalized first PC of AMOC from Fig. 1c. The variance explained by the first EOF is approximately 33 and 25%, respectively, for temperature and density. The correlation between PC1s of temperature (density) and AMOC is 0.60 (0.65). Contour intervals are 0.2°C in (**a**) and 0.02 kg m^{-3} (**b**)

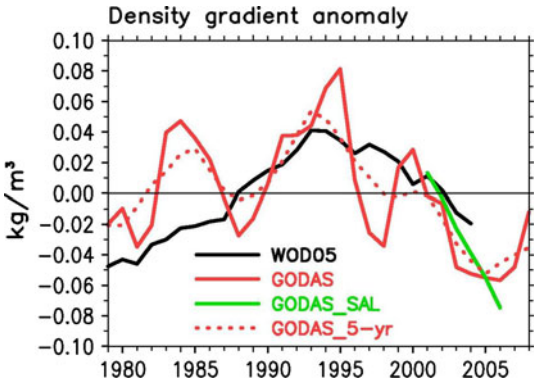

Fig. 4 Density gradient anomaly between subpolar (50°–65°N) and subtropical (30°–45°N) Atlantic in the upper 700 m in WOD05, GODAS, GODAS_SAL, and GODAS using 5-year running mean temperature and salinity. The correlation coefficient between WOD05 and GODAS is 0.68. "GODAS_5-year" indicates the gradient of density using 5-year running mean filtered temperature and salinity in GODAS

The meridional gradient of density between subpolar and subtropical Atlantic in the WOD05 (Fig. 4) is close to that in the GODAS with correlation coefficient of 0.68. The interannual variability of density is weaker in the WOD05 (Figs. 4 and 5d) because a 5-year running mean filter is applied to its temperature analysis to match with its original 5-year running mean salinity when density is calculated. This density variability is in congruence with the one using 5-year running mean filtered temperature and salinity in GODAS (GODAS_5-year in Fig. 4). The density gradient in the GODAS_5-year agrees with that in the WOA05 better, but large discrepancies exist at times, e.g. during 1983–1985, indicating large uncertainties in density analysis in the early period.

We next examine the relative contributions of temperature and salinity variations to density variations by calculating density using either temperature (Fig. 6a) or salinity (Fig. 6b) annual climatology. From 1990–1995 to 2003–2008, the density decreased dramatically north of 45°N with an amplitude of 0.12 kg m^{-3} in the upper 300 m, while it changed little south of 45°N (Fig. 6c). The decrease in density north of 45°N is largely attributed to an increase in temperature which decreased the density by as much as 0.12 kg m^{-3} in the upper 200 m (Fig. 6a). In contrast, the density south of 45°N changed little, partly due to a cancellation between an increase in density from increased salinity and a decrease in density from increased temperature. Therefore, the decrease of meridional density gradient from 1990–1995 to 2003–2008 (Fig. 4) is mostly due to the decrease of density north of 45°N (Fig. 6c), and is attributed to the decrease of temperature north of 45°N (Fig. 6a).

The above results point to a minor role of salinity in density variation, and may be biased since synthetic salinity is used in the GODAS. The WOD05, that includes observed temperature and salinity data, can be used to verify the GODAS (Fig. 7). The contribution of salinity change to density change differs significantly north of

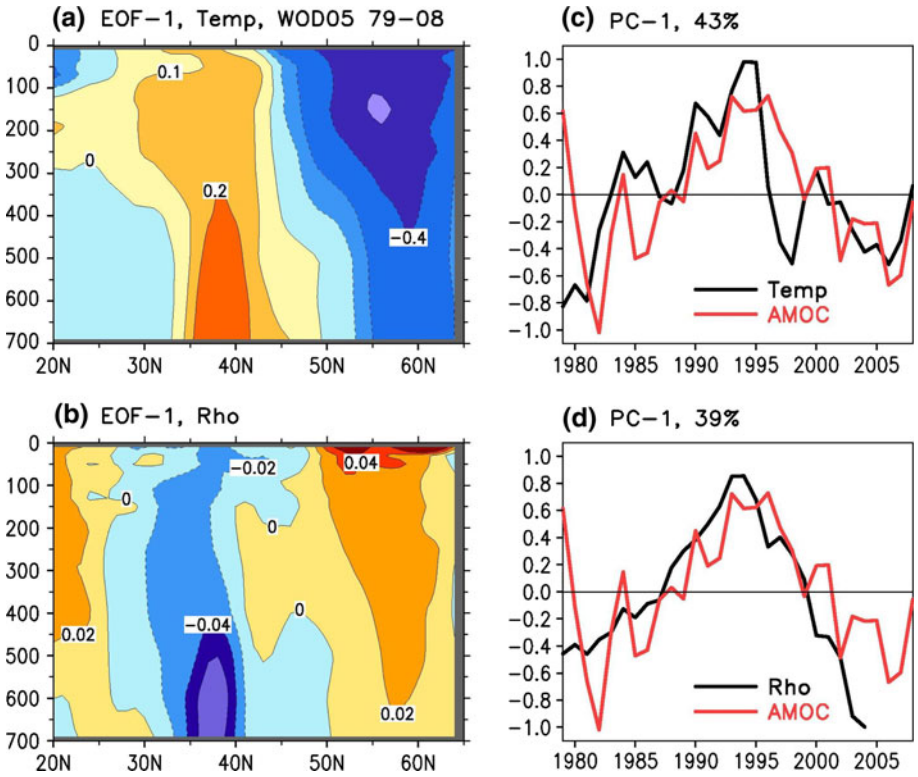

Fig. 5 Same as in Fig. 3 except for WOD05 with explained variance of approximately 43 and 39%. Correlation coefficients between WOD05 (Fig. 5) and GODAS (Fig. 4) are 0.81, 0.80, 0.68, and 0.58, respectively, in (**a**, **c**, **b**, and **d**). A 5-year running mean is first applied to the temperature and salinity data when density is calculated, and the EOF of density is then analyzed

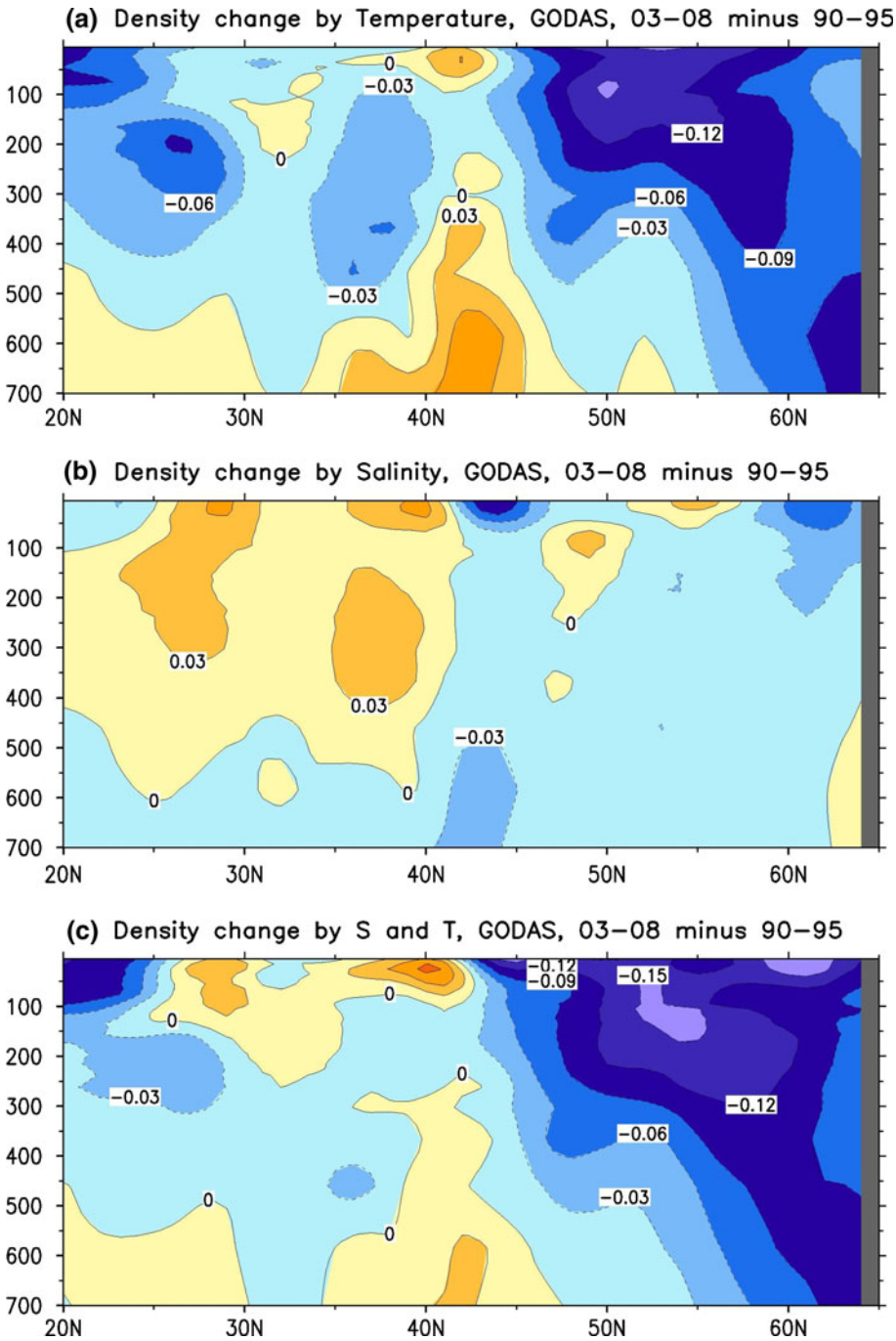

Fig. 6 Zonally averaged density changes in the North Atlantic between 2003–2008 and 1990–1995 in GODAS due to (**a**) temperature, (**b**) salinity, and (**c**) temperature and salinity. Contour intervals are 0.03 kg m^{-3}

40°N in the GODAS and WOD05 (Figs. 6b and 7b). A comparison of salinity between the two data sets indicated that the zonally averaged salinity in the high latitudes in the GODAS is above 0.15 psu too high relative to the WOD05 salinity in the upper 200 m before 1995 (not shown). So the differences in the contribution of salinity change to density change north of 40°N (Figs. 6b and 7b) are largely due to the differences in salinity analysis before 1995 when observations are very sparse. In addition, the differences may partially result from the averaged period of 2003–2004 in WOD05 and 2003–2008 in GODAS. Despite of uncertainties in salinity analysis before 1995, both the GODAS and WOD05 suggest that the temperature increase from 1990–1995 to 2003–2008 dominated the density decrease. In addition, we examined the U.K. Met Office objectively analyzed temperature and salinity analysis (EN3_v2a), and found that the above results are not sensitive to data sets used.

To further quantify the potential role of salinity in density variation and the AMOC variability, we also

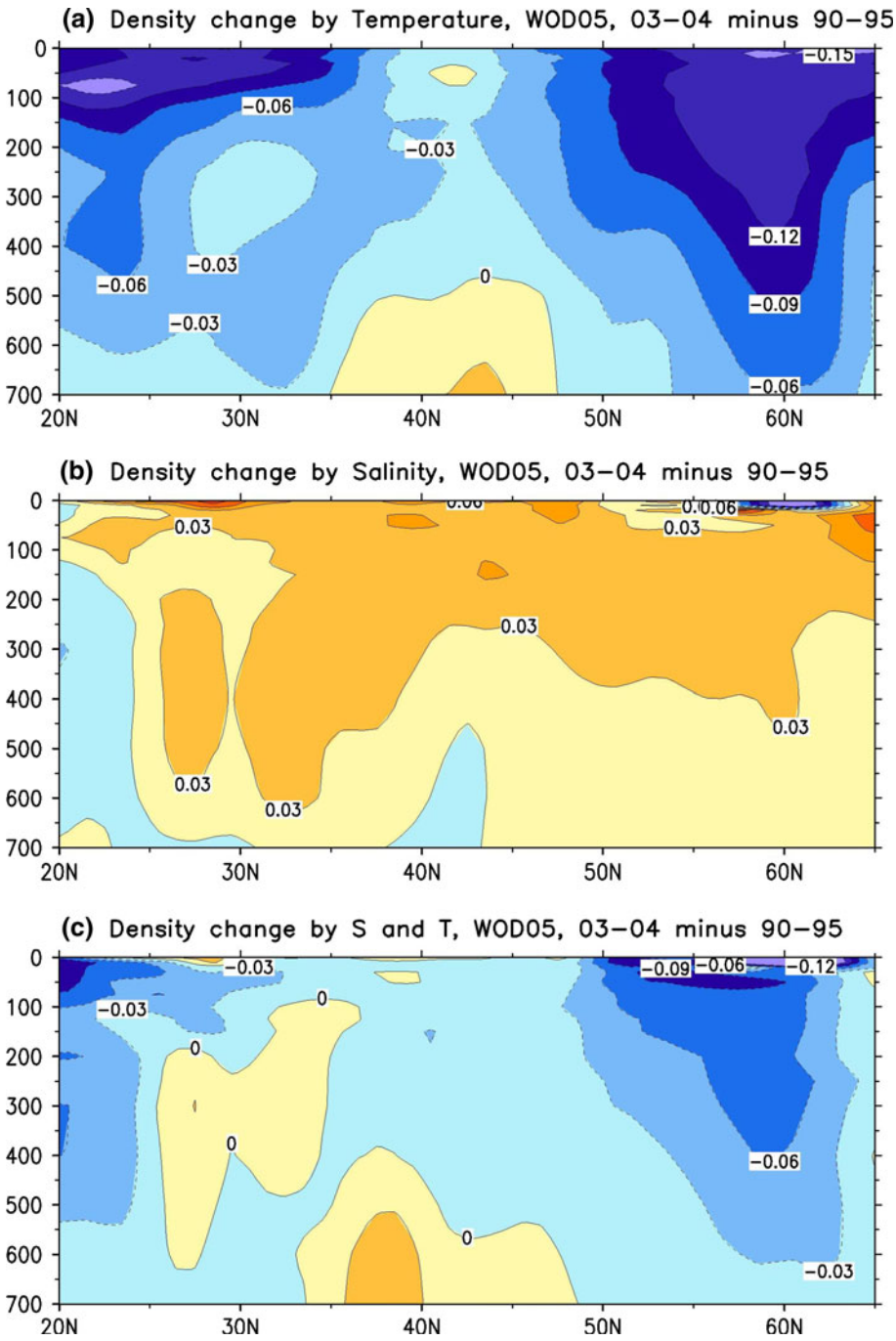

Fig. 7 Same as Fig. 6 except for WOD05

examine an experiment that assimilates both observed temperature and salinity for the period 2001–2006 (GODAS_SAL). It is interesting to note that replacing synthetic salinity with observed salinity had little impact on the AMOC variability (Figs. 1c and 2b). Also, decreasing trend in the meridional density gradient in the GODAS_SAL is quite similar to that in the GODAS. However, it remains to be seen whether salinity data could make a critical contribution to the AMOC variability in the GODAS before 2000, as suggested by Frankignoul et al. (2009). In addition, an observing system similar to Argo where temperature and salinity measurements are available up to the 2,000 m depth may be critical for a complete represent of the AMOC variability (Zhang et al. 2009).

5 The roles of atmospheric forcing and subpolar gyre on the AMOC variability

It has been argued that the variability of the AMOC in the northern North Atlantic is primarily driven by changes in deep water formation taking place in the subpolar region,

which is strongly influenced by the NAO (Eden and Willebrand 2001; Bentsen et al. 2004; Böning et al. 2006; Kuhlbrodt et al. 2007). Following this hypothesis, we will next examine the dominant variability in the net surface heat flux (HFLX, positive downward), freshwater flux E-P, and Ekman pumping (positive upward) based on the NCEP Reanalysis 2 (Kanamitsu et al. 2002), factors that are influenced by the surface atmospheric variability associated with the NAO.

The EOF1 and PC1 of HFLX and Ekman pumping account for 28 and 23% of total variance, respectively, and are largely consistent with those based on the NCEP Reanalysis 1 (Kalnay et al. 1996) discussed by Häkkinen and Rhines (2004). Figure 8a shows that the HFLX in the subpolar Atlantic is out of phase with that in the subtropical Atlantic with the largest loading in the Labrador Sea. The PC1 of HFLX is highly correlated with the wintertime (January–March) NAO index. The subpolar Atlantic warmed during early and mid-1980s, while cooled during later 1980s and early 1990 (Fig. 8a, d). The continuous weakening of the subpolar air-sea heat loss is consistent with the observations that deep convective conditions in the Labrador Sea have been absent since the early 1990s (Häkkinen and Rhines 2004). Consistent with the NAO wind pattern, the Ekman pumping is enhanced north of 55°N and suppressed in the central midlatitude North Atlantic (Fig. 8c). The PC1 of Ekman pumping is very

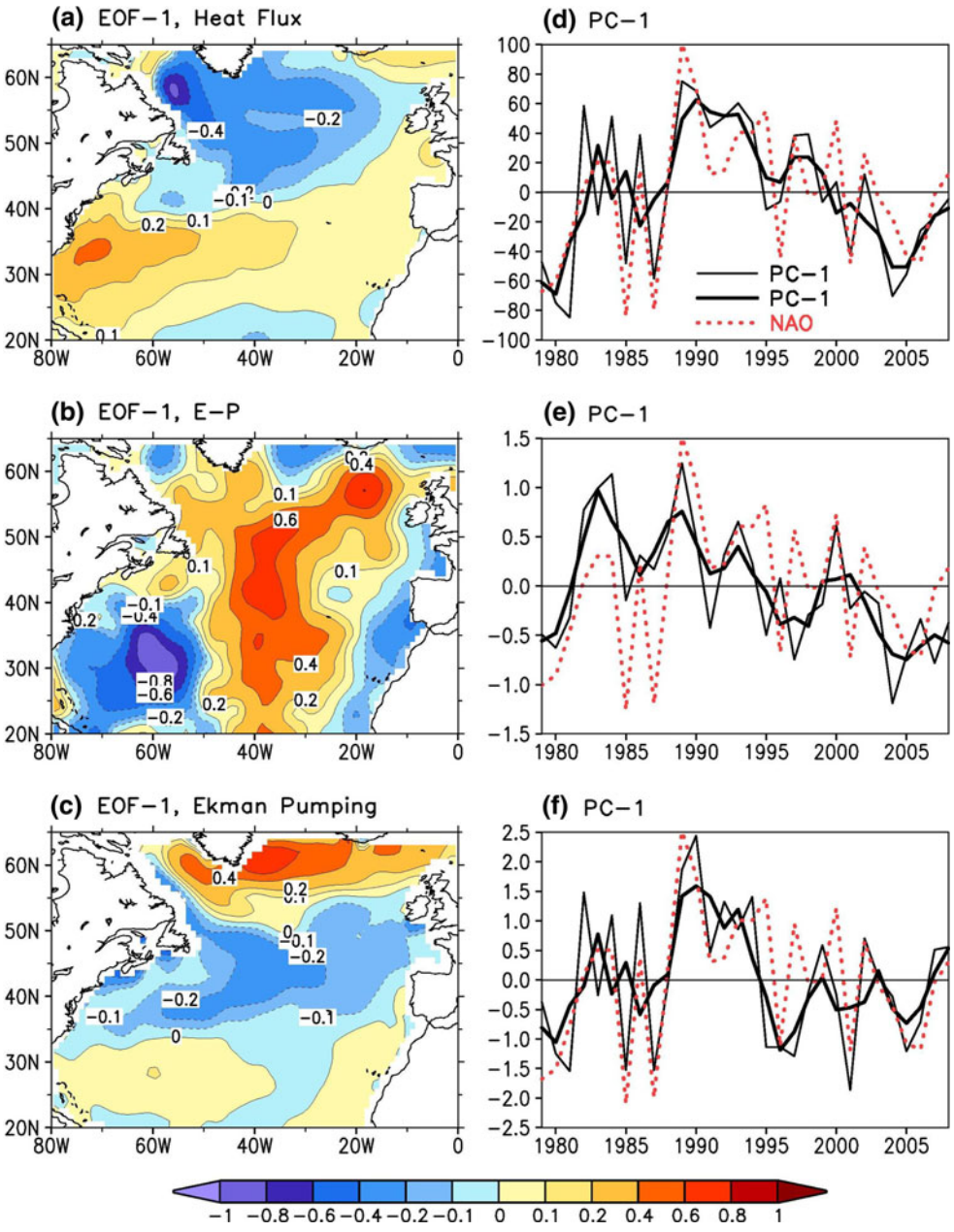

Fig. 8 First EOFs of (**a**) net surface heat flux, positive downward, (**b**) E-P, and (**c**) Ekman pumping, positive upward. The EOF1s explain 28, 15, and 23% variances, respectively. The contour intervals are 0.2 in (**a–c**). Their respective PC1s in (**d–f**) are in unit of W m^{-2}, mm/day, and m/day; the thick black lines represent a 3-year running mean of PC1s; the thick red lines represent normalized 3-year running mean NAO index of winter (January–March). The correlation coefficients between NAO and PC1s of heat flux, E-P, and Ekman pumping are 0.77, 0.47, and 0.69, respectively

similar to the PC1 of HFLX except it declined to the lowest value during 1994–1995 and had a weak upward trend from 1995 to 2008 (Fig. 8f).

The EOF1 and PC1 of freshwater flux, accounting for 15% of total variance over the analysis domain, suggests that the eastern North Atlantic east of 50°W exhibited a strong salinification tendency in early 1980s, and a reverse tendency from 1983 to 2008, and the southwestern North Atlantic had opposite tendencies. The PC1 of freshwater flux generally agrees with the NAO index during 1990–2008, but shows a clear disagreement during 1979–1989 (Fig. 8e).

The changes in surface heat flux appear to be consistent with the variations in subsurface temperature (Figs. 3c and 5c) and the AMOC (Fig. 1c). The enhanced surface cooling north of 40°N from 1979 to 1990 led to a decreased subsurface temperature and an increased AMOC from 1980 to 1995. A weakened surface cooling north of 40°N from 1990 to 2008 resulted in an increased subsurface temperature and a decreased AMOC from 1995 to 2008. The changes in surface heat flux lead the changes in subsurface temperature and AMOC about 5 years; while changes of subsurface temperature and AMOC are largely in phase. This suggests that the variations of the AMOC in the GODAS are forced by the overlaying atmospheric variability. The 5-year lag of subsurface temperature and AMOC to the surface forcing is similar to the analysis of Häkkinen and Rhines (2004) and Eden and Willebrand (2001) who suggested a 3–5 year lag of baroclinic current to surface forcing.

The net buoyancy (Gill 1982) forcings due to HFLX and E-P (positive downward) are quantified as integrated buoyancy flux north of 40°N (Fig. 9). The selection of 40°N is based on the EOF1s shown in Fig. 8a, b, and the conclusion that the AMOC is sensitive to the surface heat flux and E-P flux north of 40°N (Bunion et al. 2006). Figure 9 shows that the integrated buoyancy forcing from surface heat flux dominates over that from E-P. This agrees with the analysis in Sects. 4 and 5 that the subsurface density change north of 40°N was associated with temperature change, and the contribution from salinity was small. Numerical model experiments and observational analyses (Eden and Willebrand 2001; Häkkinen and Rhines 2004; Böning et al. 2006) also suggest that surface heat flux and wind stress curl associated with the NAO are the dominant atmospheric forcings for the decadal and multi-decadal AMOC variability in the northern North Atlantic, while the freshwater flux plays a minor role.

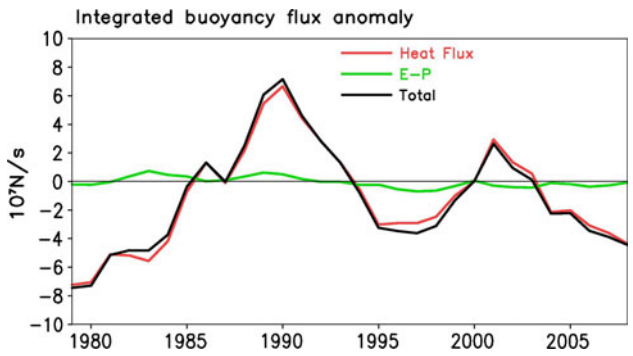

Fig. 9 Integrated buoyancy flux anomaly (positive downward) in unit of 10^7 N s^{-1} in GODAS. The buoyancy flux is integrated north of 40°N. The total buoyancy flux represents the buoyancy from both heat flux and E-P, which leads PC1 of AMOC (Fig. 1c) for 3–4 years with a correlation coefficient of 0.64. A 3-year running mean is applied in the plot

The total downward buoyancy forcing north of 40°N increased from 1979 to 1990, and decreased during 1990–1995 and 2001–2008, which led the changes in AMOC (Fig. 1c) and subsurface temperature (Figs. 3a and 5a) by 3–4 year with a correlation coefficient of 0.64. This is consistent with the analysis of coupled model outputs (Grist et al. 2009), who showed that the AMOC lags the surface density flux into the ocean by 2–3 year, while the analysis of Josey et al. (2009) suggested a longer (6–10 year) lag of AMOC to the surface density flux.

The variations of surface heat flux in the subpolar Atlantic directly impact the strength of deep convection. Ocean heat loss related to a positive NAO enhances the deep convection in the Labrador and Irminger Sea, which leads to a strengthening of the subpolar gyre (Eden and Willebrand 2001) and western boundary currents off Labrador (Häkkinen and Rhines 2004; Böning et al. 2006) after about 3 year. The AMOC variability in the northern North Atlantic tends to covary with the changes of subpolar gyre and western boundary currents off Labrador (Böning et al. 2006; Frankignoul et al. 2009). To analyze this aspect in the GODAS, we examine how well the GODAS simulates the variability in deep convection, subpolar gyre transport and western boundary currents and their lead/lag correlations with the AMOC.

The strength of deep convection can be quantified by anomalous mixed layer depth (MLD) as shown by Bentsen et al. (2004) and Böning et al. (2006). Figure 10a, c shows that winter time (Feb–Apr) MLD (the deep convection) was deeper (stronger) than normal in the Labrador and Irminger Sea before 1995, and was shallower (weaker) from 1995 to 2008. The maximum variability of MLD is over 1,000 m. The changes in deep convection may directly results in the variations in the subpolar gyre that is quantified by barotropic stream function (BSF; Fig. 10a, b). The subpolar gyre was strong in 1985 and 1995, and became weaker from 1995 to 2008. The maximum variability of the subpolar gyre is over 4 Sv. The BSF variation further results in the changes in AMOC, at 55°N for example (Fig. 10a). The MLD (deep convection) leads

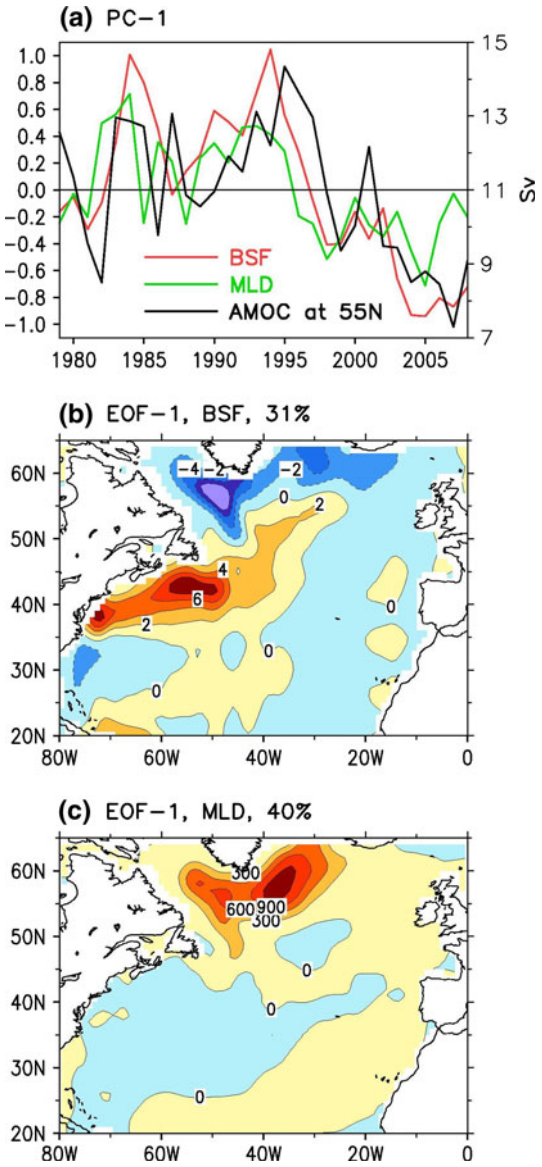

Fig. 10 **a** Normalized PC1s of BSF and MLD (*left axis*), along with maximum AMOC at 55°N (*right axis*); **b** EOF1 of BSF with a variance of 31%; and **c** EOF1 of MLD with a variance of 40%. The contour interval is 2 Sv in (**b**) and 300 m in (**c**). The correlation coefficient is 0.79 between MLD and BSF with MLD leading for 1 year, 0.61 between MLD and AMOC at 55°N with MLD leading for 3 year, and 0.78 between BSF and AMOC at 55°N with BSF leading for 1 year. Contour interval is 2 Sv in (**b**) and 300 m in (**c**)

BSF by approximately 1 year with a correlation coefficient of 0.79, and leads AMOC at 55°N by approximately 3 year with a correlation coefficient of 0.61. BSF leads AMOC at 55°N by approximately 1 year with a correlation coefficient of 0.78. These results suggest that the AMOC variability in GODAS may first be driven by surface heat flux and E-P via high latitude deep convection. The changes in deep convection directly result in variations of BSF and subsequently AMOC. This causal link between surface heat flux and AMOC is consistent with the studies of Bentsen et al. (2004), Böning et al. (2006), and the mechanisms proposed by Zhang (2008). However, the AMOC change may also be linked to the surface wind stress curl (Fig. 8c) as indicated in Böning et al. (2006). The reason is that both surface heat flux and wind are directly associated with the changes in NAO.

6 Summary and discussions

Our analysis shows that the AMOC strengthened in the GODAS from 1980 to 1995 and weakened from 1995 to 2008. The AMOC variation is associated with the subsurface temperature and density variations in the North Atlantic in the GODAS and the objective analysis of the observed hydrographic data of WOD05. Several other ocean reanalyses also show that AMOC strengthened from 1980 to 1995, and weakened after 1995 (Wunsch and Heimbach 2006; Balmaseda et al. 2007). Similarly, some ocean model simulations indicate that AMOC strengthened before 1995 and weakened after 1995 (Bentsen et al. 2004; Böning et al. 2006; Bingham et al. 2007; Frankignoul et al. 2009).

Direct AMOC observations (Fig. 2a) (Bryden et al. 2005; and Kanzow et al. 2010) suggest a weakening (strengthening) AMOC at 26.5°N after (before) 1993. The downward trend of AMOC at 26.5°N in the GODAS, however, is very weak after 1997. Recent RAPID observations (Fig. 2b) show that AMOC at 26.5°N exhibited strong seasonal and interannual variabilities from 2004 to 2008. These variabilities are well simulated by GODAS with a slightly weak mean and standard deviation, indicating a good model performance as more observed data are assimilated into the GODAS.

The magnitude of AMOC variability in the GODAS is approximately 3-4 Sv (Fig. 1b), which is comparable with the ocean synthesis estimations of Balmaseda et al. (2007) and Köhl and Stammer (2007), the simulations of Bingham et al. (2007), Frankignoul et al. (2009) and Danabasoglu (2008). But it is stronger than the simulation of Wunsch and Heimbach (2006; 2.3 Sv), the estimations of Böning et al. (2006; 1–2 Sv) and Bentsen et al. (2004; 1–2 Sv). Model simulations (Danabasoglu 2008) suggested a period of 20–80 year in AMOC variation, while it is difficult for us to estimate the period of AMOC variability in the GODAS due to limited data length.

Our analysis suggests a dominant role of subsurface temperature variation in the AMOC variability. On the other hand, modeling studies of Frankignoul et al. (2009), Msadek and Frankignoul (2009), and Zhang et al. (2009) suggested that the salinity variability contributes dominantly to the interannual-decadal variability of AMOC. The modeling study of Danabasoglu (2008) indicated an

equally important role of temperature and salinity in the variability of the AMOC. These conclusions are different from the GODAS analysis. The study of Msadek and Frankignoul (2009) indicated that density variability leads AMOC approximately 4 year. However, changes in density are in phase with AMOC in the GODAS, but density changes in the WOD05 lead the AMOC in the GODAS by 1–2 year.

It had been hypothesized that the AMOC variations could be forced by surface heat flux, E-P, and wind stresses (Kuhlbrodt et al. 2007). Our analysis based on GODAS suggests that variations in the AMOC and subsurface temperature are indeed forced by the surface heat flux and wind stresses in the North Atlantic as indicated by many earlier studies (Stommel 1961; Rahmstorf 1996; Huang et al. 2003; Bugnion et al. 2006). These variations of surface heat flux and wind stresses are also closely related to the winter NAO index as indicated by Häkkinen and Rhines (2004), which lead the AMOC variations by approximately 5-year in agreement with the GODAS analysis.

The analyses suggest that the changes in AMOC are directly associated with changes in subpolar gyre. Figure 10 shows that both subpolar gyre and AMOC at 55°N strengthened from 1986 to 1995, and weakened from 1995 to 2008. The changes in subpolar gyre can also be seen by the changes in zonal current near 45°N according to thermal wind effect (Figs. 3a and 5a). This is in concordance with the geostrophical current analysis based on altimetry sea surface height observations (Häkkinen and Rhines 2004), and a weakening deep western boundary current off Labrador since 1995 in a model simulation (Böning et al. 2006). However, Zhang (2008) argued that the weakening subpolar gyre after 1995 may be associated with a strengthening AMOC. The argument is based on (1) the AMOC is highly correlated with Atlantic Multidecadal Oscillation (AMO) in some coupled model runs (Delworth and Mann 2000; Knight et al. 2005), and (2) Observed AMO index has been strengthening since 1995 (Kerr 2000). Further studies are required to clarify the discrepancy between different analyses.

Caution is required in the interpretation of the AMOC analysis based on the GODAS since the model domain does not extend to the Arctic; No sea-ice and its influence on the fresh water budget are considered in the model; and synthetic rather than observed salinity is assimilated into the system (Behringer and Xue 2004). These deficiencies in the model could potentially underestimate the role of salinity in the AMOC variability as suggested by Jungclaus et al. (2005). The influence, however, appears not to be severe. The reasons are (1) both WOD05 and EN3 analyses also show a weak contribution of salinity to density during the past 30 year; (2) a sensitivity experiment, which assimilated observed salinity from 2001 to 2006 (GODAS_SAL), indicates that the AMOC variations in GODAS_SAL only changed slightly between 2001 and 2006; and (3) integrated surface buoyancy forcing is overwhelmingly determined by the surface heat flux and the contribution from E-P is small. It is, therefore, suggested that the role of salinity in AMOC may indeed be weak in the past decades. Since salinity from WOD05 and heat and freshwater fluxes from NCEP R2 are not direct observations, the validation of GODAS analysis using these data sets may be biased. More comparisons with direct observations and other model based analysis are expected to further clarify some of the issues.

The difference in the magnitude of AMOC variabilities between GODAS and the control simulation without data assimilation strongly suggests the important role of data assimilation in constraining the AMOC variations. The impacts of assimilation of observed temperature profiles in GODAS can reduce the temperature and density biases in the North Atlantic (not shown), and therefore reduce the model deficiencies of the artificial northern boundary excluding the Arctic and removal of the sea ice.

Given the importance of the AMOC in long-term climate variability, model estimates of AMOC based on ocean data assimilation systems are an important climate monitoring tool. Such estimates also provide a means to validate the characteristics of the AMOC in coupled model simulations. Similar analysis for the AMOC variability from ocean analyses at different operational centers will further clarify the AMOC variability and provide multi-model tools for monitoring AMOC in real time.

Acknowledgments Authors thank Tim Boyer of National Oceanographic Data Center for providing us objectively analyzed salinity and temperature data of the World Ocean Database 2005. Comments from two anonymous reviewers have greatly improved our manuscript.

References

Balmaseda MA et al (2007) Historical reconstruction of the Atlantic meridional overturning circulation from the ECMWF operational ocean reanalysis. Geophys Res Lett 34:L23515. doi:10.1029/2007GL031645

Behringer DW (2007) The global ocean data assimilation system (GODAS) at NCEP. Preprints, 11th symp. on integrated observing and assimilation systems for atmosphere, oceans, and land surface, San Antonio, TX, Amer. Meteor. Soc., 3.3. Available online at http://ams.confex.com/ams/87ANNUAL/techprogram/paper_119541.htm

Behringer DW, Ji M, Leetma A (1998) An improved coupled model for ENSO prediction and implication for ocean initialization. Part I: the ocean data assimilation system. Mon Wea Rev 126:1013–1021

Behringer DW, Xue Y (2004) Evaluation of the global ocean data assimilation system at NCEP: the Pacific ocean. Eighth symposium on integrated observing and assimilation system for atmosphere, ocean, and land surface, AMS 84th annual meeting,

Washington State Convention and Trade Center, Seattle, Washington, pp 11–15
Bentsen M et al (2004) Simulated variability of the Atlantic meridional overturning circulation. Clim Dyn 22:701–720
Bingham RJ et al (2007) Meridional coherence of the North Atlantic meridional overturning circulation. Geophys Res Lett 34:L23606. doi:10.1029/2007GL031731
Böning CW et al (2006) Decadal variability of subpolar gyre transport and its reverberation in the North Atlantic overturning. Geophys Res Lett 33:L21S01. doi:10.1029/2006GL026906
Boyer TP et al (2006) World Ocean database 2005. In: Levitus S (ed) NOAA atlas NESDIS, vol 60. U.S. Government Print Office, Washington, DC, 190 pp
Bryden HL et al (2005) Slowing of the Atlantic meridional overturning circulation at 25 N. Nature 438. doi:10.1038/nature04385
Bugnion V et al (2006) An adjoint analysis of the meridional overturning circulation in an ocean model. J Clim 19:3732–3750
Cunningham SA, Kanzow T, Rayner D, Baringer MO, Johns WE, Marotzke J, Longworth HR, Grant EM, Hirschi JJ-M, Beal LM, Meinen CS, Bryden HL (2007) Temporal variability of the Atlantic meridional overturning circulation at 26.5°N. Science 317:935–938. doi:10.1126/science.1141304
Danabasoglu G (2008) On multidecadal variability of the Atlantic meridional overturning circulation in the community climate system model version 3. J Clim 21:5524–5544
Delworth TL, Mann ME (2000) Observed and simulated multidecadal variability in the Northern Hemisphere. Clim Dyn 16:661–676
Eden C, Willebrand J (2001) Mechanism of interannual to decadal variability of the North Atlantic circulation. J Clim 14:2266–2280
Frankignoul C, Deshayes J, Curry R (2009) The role of salinity in the decadal variability of the North Atlantic meridional overturning circulation. Clim Dyn. doi:10.1007/s00382-008-0523-2
Gill AE (1982) Atmosphere-ocean dynamics. Academic Press, Cambridge
Grist JP, Marsh R, Josey SA (2009) On the relationship between the North Atlantic meridional overturning circulation and the surface-forced overturning stream function. J Clim 22:4989–5002
Häkkinen S, Rhines PB (2004) During the 1990s decline of subpolar North Atlantic circulation. Science 304. doi:10.1126/science.1094917
Held IM et al (2005) Simulation of Sahel drought in the 20th and 21st centuries. PNAS 102:17891–17896. doi:10.1073/pnas.0509057102
Huang B, Stone PH, Hill C (2003) Sensitivities of deep-ocean heat content to surface fluxes and subgrid-scale parameters in an ocean general circulation model. J Geophys Res 108. doi:10.1029/2001JC001044
Huang B, Xue Y, Behringer DW (2008) Impacts of Argo salinity in NCEP global ocean data assimilation system: the tropical Indian ocean. J Geophys Res 113:C08002. doi:10.1029/2007JC004388
Josey SA, Grist JP, Marsh R (2009) Estimates of meridional overturning circulation variability in the North Atlantic from surface density flux fields. J Geophys Res 114:C09022. doi:10.1029/2008JC005230
Jungclaus JH, Haak H, Latif M, Mikolajewicz U (2005) Arctic North Atlantic interactions and multidecadal variability of the meridional overturning circulation. J Clim 18:4013–4031
Kalnay E et al (1996) The NCEP/NCAR 40-year reanalysis project. Bull Am Meteor Soc 77:437–470
Kanamitsu M, Ebisuzaki W, Woolen J, Yang S-K, Hnilo JJ, Fiorino M, Potter GL (2002) NCEP-DOE AMIP-II reanalysis (R-2). Bull Am Meteor Soc 83:1631–1643
Kanzow T et al (2010) Seasonal variability of the Atlantic meridional overturning circulation at 26.5°N. J Clim 23:5678–5698
Keenlyside NS et al (2008) Advancing decadal-scale climate prediction in the North Atlantic sector. Nature 453:84–88. doi:10.1038/nature06921
Kerr RA (2000) A North Atlantic climate pacemaker for the centuries. Science 288:1984–1985
Knight JR, Allan RJ, Folland CK, Vellinga M, Mann ME (2005) A signature of persistent natural thermohaline circulation cycles in observed climate. Geophys Res Lett 32:L20708. doi:10.1029/2005GL024233
Köhl A, Stammer D (2007) Variability of the meridional overturning in the North Atlantic from the 50 years GECCO state estimation. Rep. 43, Institut fur Meereskunde, University of Hamburg, 38 pp
Kuhlbrodt K et al (2007) On the driving processes of the Atlantic meridional overturning circulation. Rev Geophys 45: RG2001. doi:10.1029/2004RG000166
Meehl GA et al (2009) Decadal prediction. Bull Am Metrol Soc 90:1467–1485
Msadek R, Frankignoul C (2009) Atlantic multidecadal oceanic variability and its influence on the atmosphere in a climate model. Clim Dyn 33:45–62. doi:10.1007/s00382-008-0452-0
Pohlmann H, Jungclaus JH, Köhl A, Stammer D, Marotzke J (2009) Initializing decadal climate predictions with the GECCO oceanic synthesis: effects on the North Atlantic. J Clim 22:3926–3938
Rahmstorf S (1996) On the freshwater forcing and transport of the Atlantic thermohaline circulation. Clim Dyn 12:799–811
Smith DM et al (2007) Improved surface temperature prediction for the coming decade from a global climate model. Science 317. doi:10.1126/science.1139540
Stommel H (1961) Thermohaline convection with two stable regimes of flow. Tellus 13B:224–230
Vellinga M (1996) Instability of two-dimensional thermohaline circulation. J Phys Oceanogr 26:305–319
Wang C et al (2009) Seawater density variations in the North Atlantic and the Atlantic meridional overturning circulation. Clim Dyn 33. doi:10.1007/s00382-009-0560-5
Wunsch C (2005) Thermohaline loops, Stommel box models, and the Sandstrom theorem. Tellus 57A:84–99
Wunsch C, Heimbach P (2006) Estimated decadal changes in the North Atlantic meridional overturning circulation and heat flux 1993–2004. J Phys Oceanogr 36:2012–2024
Zhang R (2008) Coherent surface subsurface fingerprint of the Atlantic meridional overturning circulation. Geophys Res Lett 35:L20705. doi:10.1029/2008GL035463
Zhang S, Rosati A, Harrison MJ (2009) Detection of multidecadal oceanic variability by ocean data assimilation in the context of a "perfect" coupled model. J Geophys Res 114: C12018. doi:10.1029/2008JC005261